

# Resonant Kelvin-Helmholtz modes in sheared relativistic flows

Manuel Perucho<sup>1,4</sup>, Michał Hanasz<sup>2</sup>, Jose-María Martí<sup>1</sup>, Juan-Antonio Miralles<sup>3</sup>

<sup>1</sup> Departament d'Astronomia i Astrofísica, Universitat de València, Spain

<sup>2</sup> Toruń Centre for Astronomy, Nicolaus Copernicus University, Toruń, Poland

<sup>3</sup> Departament de Física Aplicada, Universitat d'Alacant, Spain

<sup>4</sup> Max-Planck-Institut für Radioastronomie, Bonn, Germany

## Abstract

We announce the discovery of a new kind of high-order resonant Kelvin-Helmholtz modes acting on relativistic sheared flows which have the largest linear growth rates and crucially dominate the global stability properties of the flow in the non-linear regime. These modes were overlooked by previous studies that focused on non-relativistic relative flow speeds, infinitely thin transition layers, or very-low-order perturbation modes. The new modes grow up very fast in the linear regime, form small-scale shock fronts and then dissipate forming a relativistically hot sheath surrounding the jet core. The modification of the background flow by these modes leads to the stabilization of other disruptive modes of Kelvin-Helmholtz instability. Numerical simulations show that high Lorentz-factor jets developing these modes are exceptionally stable in the non-linear regime. The potential connection of the development of these stabilizing modes in relativistic jets with the FRI/FRII morphological dichotomy of extragalactic radio sources is suggested.

## 1 Introduction

Jets observed in a wide range of electromagnetic spectrum represent variety of morphological properties. One of the long-standing questions is related to the physical origin of the FRI and FRII dichotomy found by Fanaroff and Riley [1].

The Kelvin-Helmholtz (KH) instability (in the simplest case, that of a tangential discontinuity of velocity at the interface of parallel flows) is one of the classical instabilities of fluid dynamics [2]. We investigate the KH instability in relativistic sheared jets and address the question of the role of shear layer for the long-term evolution of relativistic extragalactic jets [3].

## 2 Method

We consider a 2D relativistic slab jet, described by relativistic equations of hydrodynamics, in Cartesian coordinates flowing along the  $z$ -coordinate and surrounded by a denser and colder ambient medium. An ideal gas equation of state with adiabatic exponent  $\Gamma = 4/3$  is applied for both the jet and ambient medium.

Both media are in pressure equilibrium and are separated by a smooth shear layer of the form:  $a(x) = a_\infty + (a_0 - a_\infty) / \cosh(x^m)$ , where  $a(x)$  represents the jet velocity  $v_z$  and the rest mass density  $\rho$  and  $a_0$  and  $a_\infty$  are their values at the jet symmetry plane (at  $x = 0$ ) and at  $x \rightarrow \infty$ . The integer  $m$  controls the shear layer steepness. In the limit  $m \rightarrow \infty$  the configuration tends to the vortex-sheet (discontinuous velocity profile) case.

We perform the linear stability analysis by imposing perturbations  $\propto F(x) \exp(i(k_z z - \omega t))$  on top of the unperturbed flow, where  $\omega$  and  $k_z$  ( $k_x$ ) are the frequency and wavenumber components along (across) the jet flow. The linearized set of relativistic equations can be reduced to a single second order ordinary differential equation for the pressure perturbation,  $P_1$  [4]

$$P_1'' + \left( \frac{2\gamma_0^2 v_{0z}' (k_z - \omega v_{0z})}{\omega - v_{0z} k_z} - \frac{\rho_{e,0}'}{\rho_{e,0} + P_0} \right) P_1' + \gamma_0^2 \left( \frac{(\omega - v_{0z} k_z)^2}{c_{s,0}^2} - (k_z - \omega v_{0z})^2 \right) P_1 = 0 \quad (1)$$

where  $c_s$  is the relativistic sound speed. Subscript 0 represents the equilibrium quantities and the prime denotes the  $x$ -derivative. The solutions (oscillation frequency  $\omega_r$  and the growth rate  $\omega_i$  vs. wavenumber  $k$ ) of the equation (1) supplemented with an appropriate set of boundary conditions [7] are found with the aid of the shooting method [5, 6].

In addition to the linear stability analysis we perform a series of numerical simulations using a finite-difference code based on a high-resolution shock-capturing scheme which solves the equations of relativistic hydrodynamics written in conservation form [8]. The numerical simulations of sheared jets for a large set of jet parameters allow us to follow the nonlinear evolution of the instability modes found with the aid of linear stability analysis.

## 3 Results

We have solved the linear problem for about 20 models (see [7]) with different specific internal energies of the jet, Lorentz factors and shear layer widths, fixing jet/ambient rest-mass density contrast ( $= 0.1$ ). We used  $m = 8, 25, 2000$  (shear layer width,  $d \approx 0.6, 0.18, 5 \cdot 10^{-3} R_j$ ;  $R_j$  is the initial jet radius) and vortex sheet for jets having specific internal energies  $\varepsilon_j = 0.4c^2$  (models B) and  $60c^2$  (models D) and Lorentz factors  $\gamma_j = 5$  (B05, D05), 10 (B10, D10) and 20 (B20, D20).

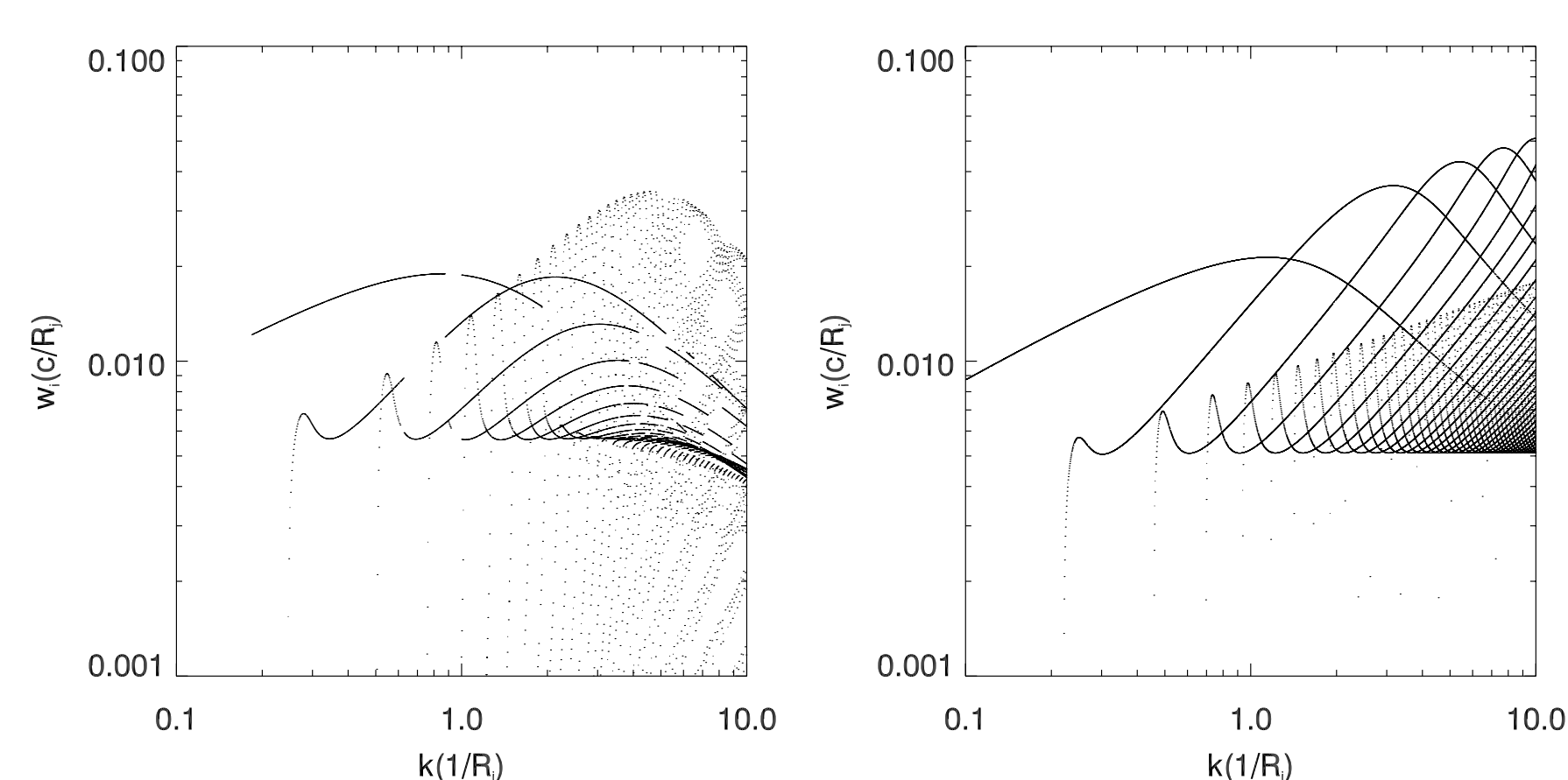


Figure 1: Growth rate vs. longitudinal wavenumber for Model D20, using a shear layer with  $m = 25$  (left panel) and vortex sheet (right panel) for the antisymmetric modes. The main difference between both cases is the overall decrease of growth rates in the sheared case, and the appearance of sharp resonances dominating over other modes.

Exemplary solutions of the linearized problem are shown in Fig. 1, where we compare the growth rates of KH instability modes vs. wavenumber  $k$  for the sheared jet boundary ( $m = 25$ ) and the vortex-sheet case ( $m = 2000$ ) for a hot and fast jet D20 (with specific internal energy density  $\sim 60c^2$  and Lorentz factor  $\gamma = 20$ ). The growth rate curves corresponding to a single mode consists on a broad maximum at larger wavenumbers and a local peak which is placed in the small wavenumber limit, near the marginal stability point of the mode (see Fig. 2). While in the vortex-sheet, relativistic case the small wavenumber peaks are relatively unimportant, in the presence of the shear layer they significantly dominate over other modes for large wavenumbers.

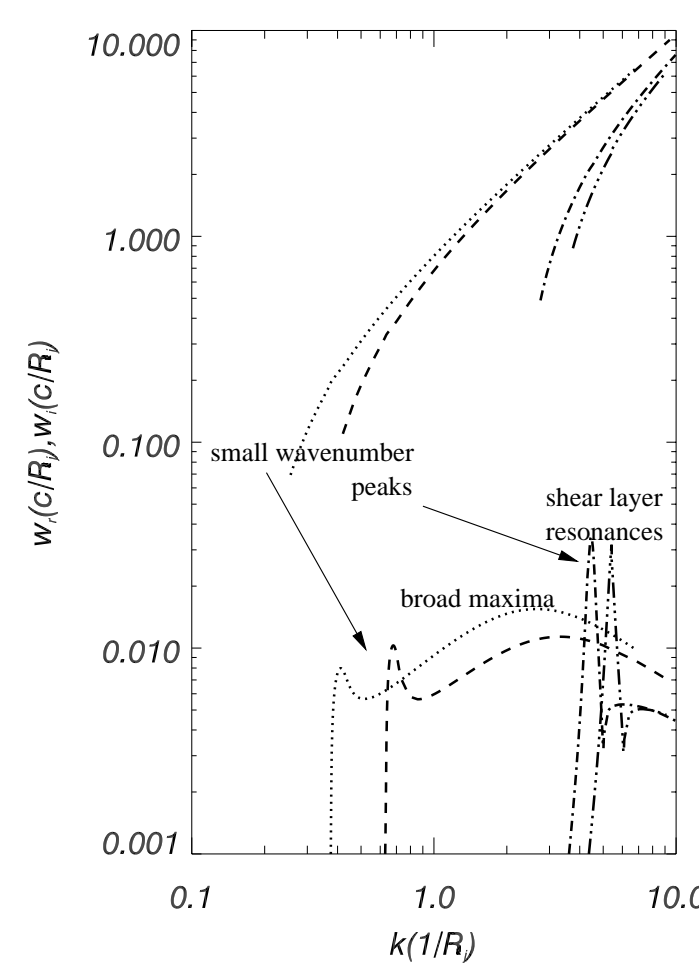


Figure 2: The structure of four modes extracted from the left panel of Fig. 1. Growth rates (lower curves) together with oscillation frequencies (upper curves) are shown. Small wavenumber peaks of high order modes show larger growth rates and are referred to as *shear layer resonances*.

The shear layer resonances correspond to very distinct spatial structures of eigenmodes, as it is seen in Fig. 3 for Model D20. In the shear layer case (central panel), the most unstable resonant modes have a small transversal wavelength which is comparable to the width of the shear layer. In the right panel of Fig. 3 we display an analogous pressure map resulting from a numerical hydrodynamical simulation.

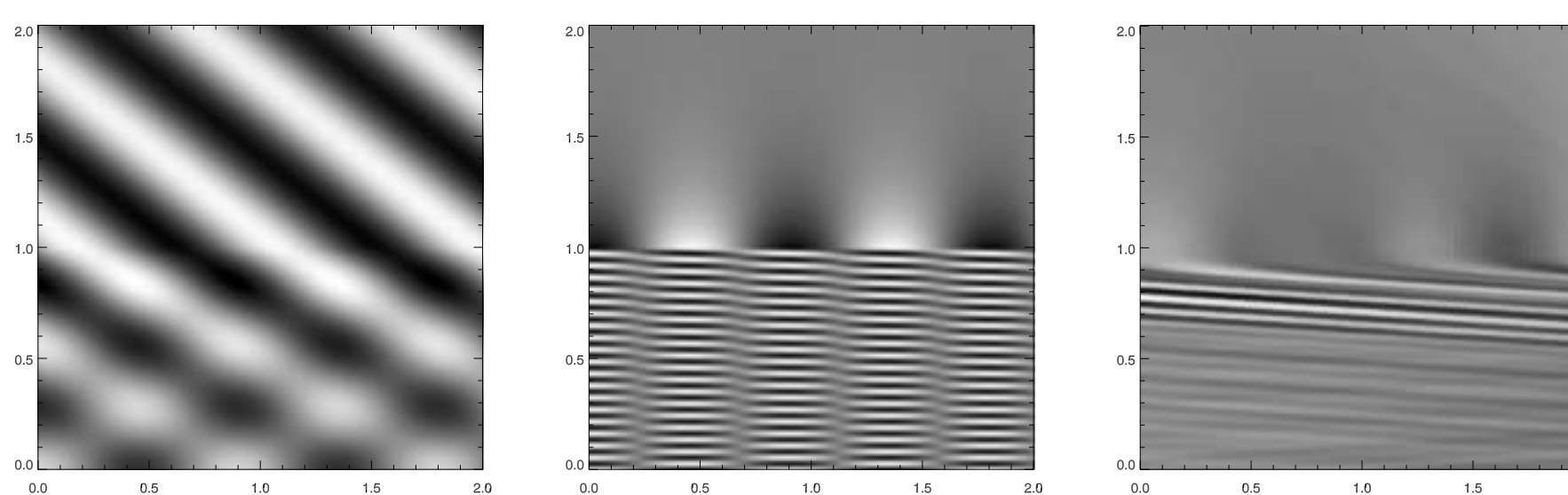


Figure 3: Pressure maps of eigenmode structures for Model D20. Left panel: the dominating mode for the vortex-sheet case. Central panel: the dominant mode for  $m = 25$  shear layer. Right panel: Pressure perturbation map from the corresponding  $m = 25$  hydrodynamical simulation.

The nonlinear evolution of the shear layer resonances, studied with the aid of numerical simulations, reveals that these modes are highly dissipative - due to the wave steepening they form shocks within the thin layer adjacent to the jet boundary. These shocks heat up the jet boundary, what is apparent in plots of the specific internal energy, which is shown along with other quantities in Fig. 4 (dashed line). The width of the hot boundary layer coincides very well with the penetration depth of the waves excited at the jet boundary.

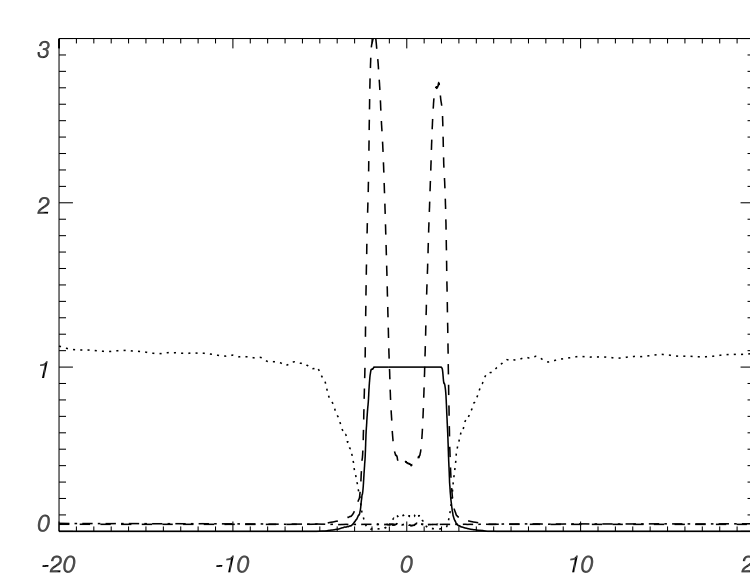


Figure 4: Averaged transversal structure in the final state of the jets corresponding to model D10. Solid line - tracer; dotted line - rest mass density; dashed line - specific internal energy. Specific internal energy has been divided by 100 to fit in the scale. The double peak in the profile of specific internal energy results from the sound wave dissipation.

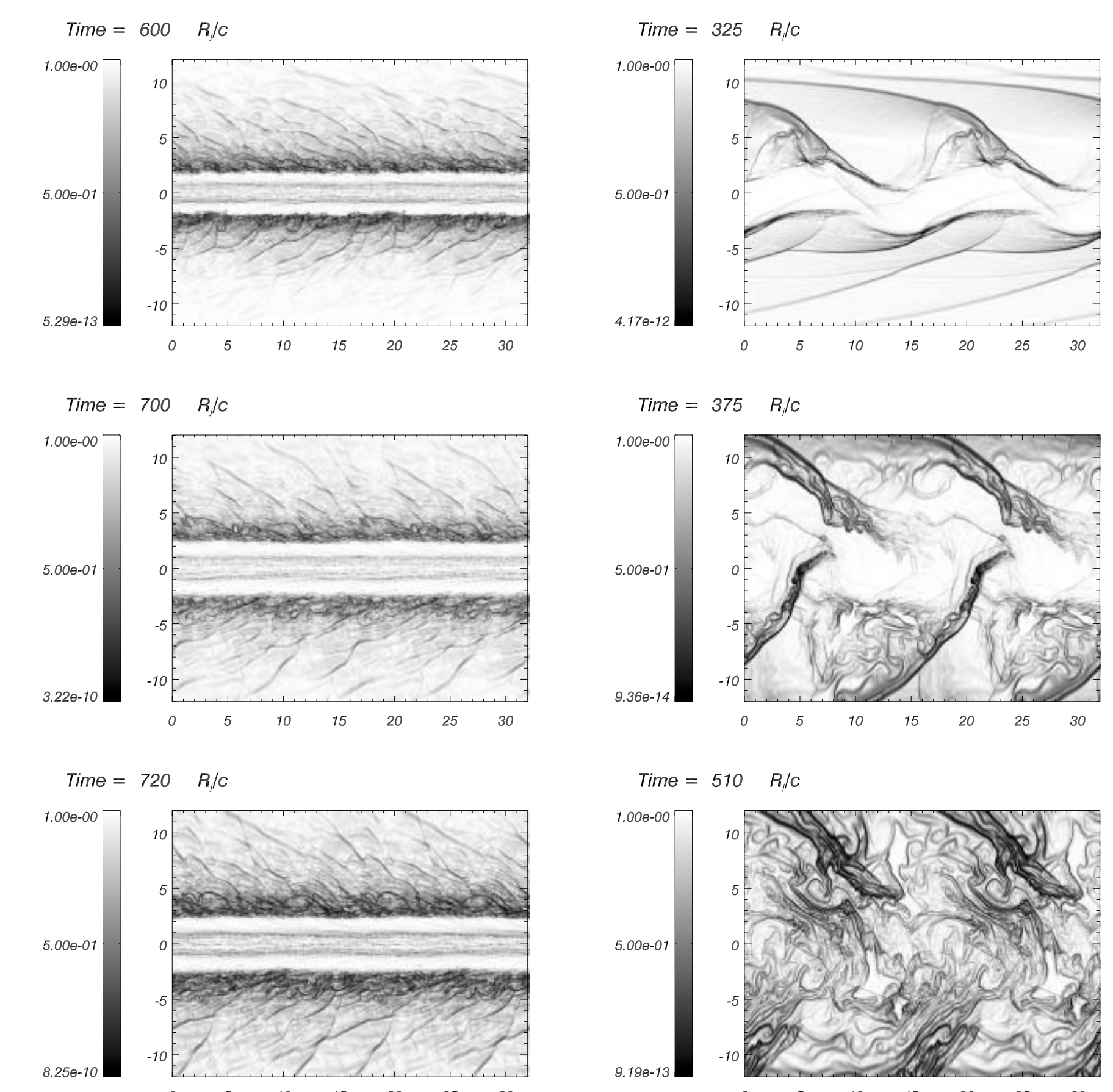


Figure 5: Schlieren plots in the non-linear regime for models B20 (left panels) and B05 (right panels). Shear layer resonances shield the jet in model B20 against disruption.

## 4 Conclusion

The importance of the shear-layer resonant modes relies not only on their dominance among solutions of the linearized problem.

We find that those jets for which the resonant modes start to dominate early in the simulation, do not disrupt and are very stable during the nonlinear evolution. An example of this behaviour is shown in Fig. 5, left column of jet maps obtained for the model B20, at three different time instants. We show also another case B05, for which the shear layer resonant modes do not develop. Jets of this type undergo strong sideway oscillations which lead to strong oblique shocks and a subsequent sudden jet disruption.

**We find therefore that the shear layer resonant modes shield jets against disruption. The shear-layer resonant modes, characterized by short radial wavelengths, suppress the growth of the disruptive long-wavelength instability modes.**

Finally, we note that the steadiness of jets developing the shear layer resonant modes makes them firm candidates to remain collimated through long distances. Hence our results would point to high Lorentz factor ( $\gamma \geq 10$ ), highly supersonic jets as forming FRII Class, whereas FRI jets would be found in the opposite limit of slow and small Mach number jets.

## References

- [1] B.L. Fanaroff, J.M. Riley, (1974) MNRAS, **278**, 586
- [2] S. Chandrasekhar, *Hydrodynamic and hydromagnetic stability*, Clarendon Press 1961; A.E. Gill, Phys. Fluids **8**, 1428 (1965); R.A. Gerwin, Rev. Mod. Phys. **40**, 652 (1968)
- [3] M. Birkinshaw, MNRAS **252**, 505 (1991); M. Hanasz and H. Sol, Astron. Astrophys. **315**; V. Urpin, Astron. Astrophys. **385**, 14 (2002); 355 (1996); P.E. Hardee and P.A. Hughes, Astrophys. J., **583**, 116 (2003), A. Ferrari et al., MNRAS **198**, 1065 (1982)
- [4] The equation was first derived by M. Birkinshaw, MNRAS **208**, 887 (1984)
- [5] W.H. Press et al., *Numerical recipes*, Cambridge Univ. Press 1997
- [6] S. Roy Choudhury and R.V.E. Lovelace, Astrophys. J. **283**, 331 (1984)
- [7] The notation for the models follows that of M. Perucho et al., Astron. Astrophys. **427**, 415 (2004a), M. Perucho et al., Astron. Astrophys. **427**, 431 (2004b), M. Perucho et al., Astron. Astrophys. **443**, 863 (2005)
- [8] J.M. Martí et al., Astrophys. J. **479**, 151 (1997).